

CLOUD SCREENING METHOD FOR OCEAN COLOR OBSERVATION BASED ON THE SPECTRAL CONSISTENCY

H. Fukushima^{a*}, K. Ogata^a, M. Toratani^a

^aSchool of High-technology for Human Welfare, Tokai University, Numazu, 410-0395 Japan
hajime@wing.ncc.u-tokai.ac.jp

Commission VIII, WG VIII/9

KEYWORDS: Algorithms, Sea, Multispectral, Underwater, Error, Detection, Quality

ABSTRACT:

The study discusses a new supplementary method of masking cloud-affected pixels in satellite ocean color imageries. Pixels, typically found around cloud edge, sometimes have anomalous features either in chlorophyll a concentration or in-water reflectance estimates caused by residual error of inter-band registration correction, or more generally, by differences in the band-wise field-of-view of the detectors. Our method is to check the pixel-wise consistency over the spectral water reflectance R_w retrieved by the atmospheric correction. We define two spectral ratio between water reflectance, IRR1 and IRR2, each defined as $R_w(B1)/R_w(B3)$ and as $R_w(B2)/R_w(B4)$ respectively, where B1~B4 stand for 4 consecutive visible bands. We show that almost linear relation holds over log-scaled IRR1 and IRR2 for ship-measured R_w data of SeaBAM in situ data set. Similar relation with a little more variability is also shown for SeaWiFS and GLI Level 2 sub-scenes. We then introduce a new cloud screening criterion that identifies those pixels that have significant discrepancy from the relationship. We apply this method to ADEOS-II/GLI ocean color data to evaluate the performance over Level-2 data, showing that it saves significant portion of near-cloud pixels yet giving chlorophyll a concentration averages in the near-cloud area that is very close to the ones in "far-cloud" pixels, or pixels that are 5 or more pixels far from the cloud edge. The method will be applicable to other satellite ocean color sensors.

1. INTRODUCTION

"Cloud screening", or identifying cloud pixels to exclude from the intended data analysis, is an important practice in satellite ocean color remote sensing as well as other earth surface remote sensing. "Simple threshold" method is considered to be most effective for ocean color cloud screening. For example, the standard cloud screening method of Sea Wide Field-of-View Scanner (SeaWiFS) data processing with SeaWiFS Data Analysis System (SeaDAS) [Fu. et al, 1998] is simply to mask the pixel if Rayleigh-corrected reflectance at near-infrared band (865nm band in this case) exceeds cloud threshold. The simple threshold method works quite successful because the cloud pixel is easily identified by its high reflectance over dark ocean.

For standard data processing of Japanese ocean color sensors, namely Ocean Color and Temperature Scanner (OCTS) aboard ADEOS, and Global Imager (GLI) aboard ADEOS-II, we have added "local variance" method to screen "noisy" pixels that are mostly found along cloud edge. The more population of these noisy pixels compared to SeaWiFS data is explained by residual error in inter-band registration correction, which is mechanically inevitable for OCTS and GLI. While other ocean color sensors may not suffer from much, derived data may possibly include similar noise pixels due to inter-band detector alignment offset.

Although the local variance method is useful, it has a tendency to mask many "valid pixels" while still leaving some noisy pixels especially on the derived chlorophyll a concentration (Chl-a) imageries. To overcome this, we propose a different approach in this paper, which utilize the spectral smoothness of the water reflectance. In the following sections, we first

introduce a spectral relationship that holds over GLI- derived cloud-free water reflectance estimates, as well as over ship-measured water reflectance data. Based on the analysis, we define the screening criterion and applied the new method to GLI data to evaluate the effectiveness.

2. SPECTRAL RELATIONSHIP OVER WATER REFLECTANCES

2.1 ANOMALOUS NEAR-CLOUD PIXELS

For this study we mainly use 1km spatial resolution data (FR data) of ADEOS-II GLI that was launched in early 2003 and was operated during April-November, 2003. It was designed for global observation of ocean, land, atmosphere and cryosphere with its 36 bands with 250m / 500m / 1km spatial resolution, covering ultra-violet, visible, near-infrared, short and long-infrared spectra [Murakami et al, 2005]. Chlorophyll a concentration (Chl-a) is estimated from atmospherically-corrected water reflectance estimates at 443, 460, 520, and 545nm bands, using following equation [Fukushima et al., 2005].

$$Chl - a = 10^{(a_1 + a_2 \times R + a_3 \times R^2 + a_4 \times R^3)} + a_5,$$

where

$$R = \frac{\max\{nLw(443), nLw(460), nLw(520)\}}{nLw(545)} \quad (1)$$

and

$$a = [0.5311, -3.559, 4.488, -2.169, -0.230].$$

Figure 1 illustrates a problem in cloud screening where noisy pixels are found around cloud area. The image is an enlarged

* Corresponding author.

portion of Chl-a image derived from a South Pacific GLI data taken on May 3, 2003. Here, cloud pixels (in black) are identified by the standard GLI cloud masking method which consists of pixel-wise "simple threshold" and 3*3 "local variance" technique over aerosol reflectance at 865nm band. Cloud-adjacent pixels, or the pixels adjacent to the "cloud pixels", are also masked.

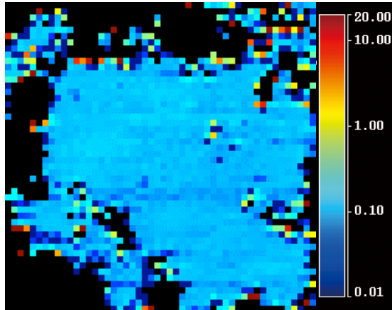


Figure 1. Cloud-screened Chl-a [µg/l] imagery of GLI data, a South Pacific scene of May 3, 2003. Noisy pixels are seen around the edge of the cloud (black pixels).

These noisy pixels are caused by "unsmooth" satellite-derived water reflectance spectrum. As one can expect, water reflectance varies systematically with the change in water constituent. It should have "smooth" spectral shape as illustrated in Figure 2 (a), where the data are sampled at pixels more than five pixels away from the cloud edge. On the contrary, "near-cloud" pixels tend to show "zig-zag" features in water reflectance spectra (b). The new method we are to propose in this study is based on the idea to detect this un-smoothness, utilizing an inter-band relationship of the spectral water reflectances at four visible bands which are typically used to estimate chlorophyll a concentration.

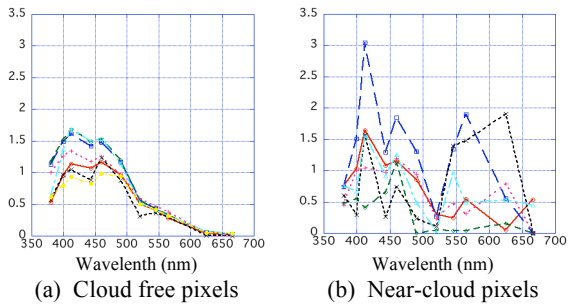


Figure 2. Example of GLI-derived normalized water-leaving radiance spectra (in µW/cm2/nm/sr) taken from a Pacific scene on June 6, 2003.

2.2 Spectral relationship over water reflectances

Figure 3 (a), which is composed from SeaBAM (SeaWiFS Bio-optical Algorithm Mini-workshop) data set [O'Reiley et al, 1998], shows a relation between two different spectral ratios of water reflectances, $Rrs(490)/Rrs(555)$ and $Rrs(443)/Rrs(510)$, where $Rrs(\lambda)$ is defined by

$$Rrs(\lambda) = \frac{L_w(\lambda)}{E_d(\lambda)} \quad (2)$$

Here, λ is wavelength, L_w is water-leaving reflectance and E_d is downward solar irradiance just above the ocean surface. Figure 3 (a) depicts a two-dimensional histogram of about one

thousand in situ data, where the distribution density is color-coded and normalized by the maximum density. Although it is true that the SeaBAM data set consists of mostly samples from Case 1 waters, all the data points are very closely distributed to the linear fit.

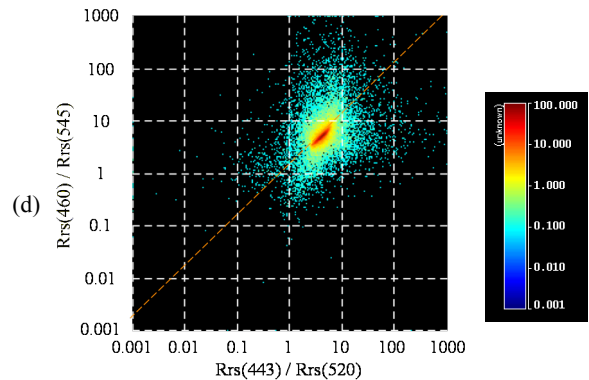
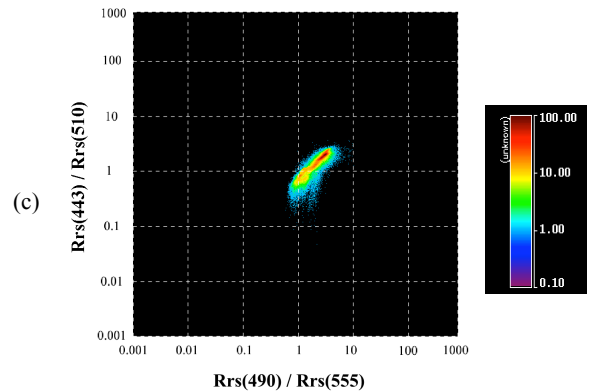
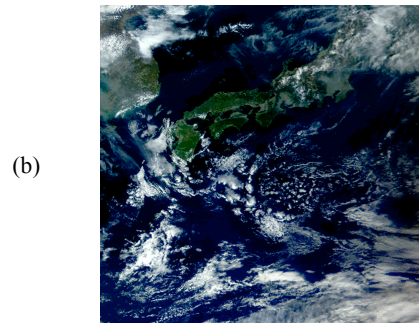
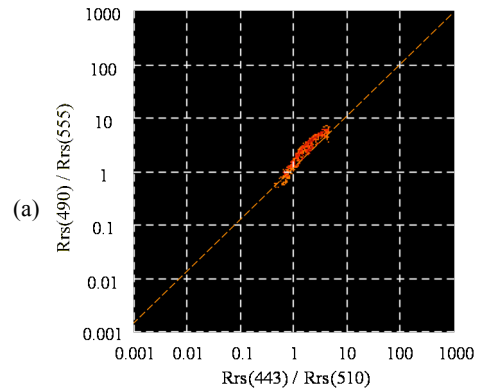


Figure 3. Inter-band relation of remote sensing reflectance. (a) SeaBAM in situ data set. (b) SeaWiFS data of April 17, 2003. (c) Inter-band relation of the SeaWiFS data. (d) The same but for GLI South Pacific scene of June 6, 2003.

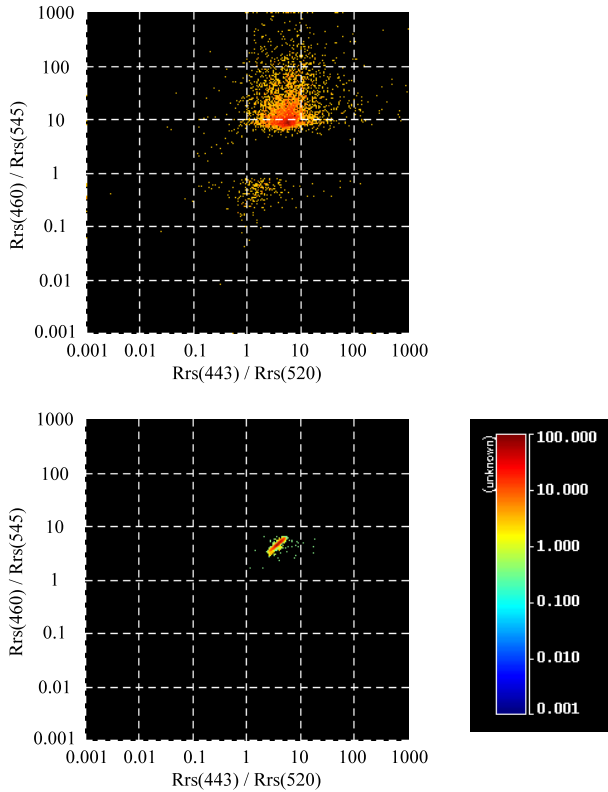


Figure 4. Inter-band relation of remote sensing reflectance on GLI South Pacific scene of June 6, 2003. (a) Cloud-adjacent pixels with Chl-a > 10.0 or with Chl-a < 0.01 µg/l. (b) Far-cloud pixels with 0.05 < Chl-a < 10 µg/l.

Similar distributions are obtained in the satellite-estimated water-reflectance spectra. Figure 3 (b) shows RGB imagery of a SeaWiFS scene of April 17, 2003 and the IRR1 and IRR2 distribution is depicted in panel (c). Figure 3 (d) is a similar plot but for the samples taken from a South Pacific scene of GLI, obtained on June 6, 2003. Note that the band selection is slightly changed because of the different band allocation of GLI. The figure shows high correlation similar to the SeaBAM and the SeaWiFS cases but with more scatterance, which should correspond to the pixels with the anomalous water reflectance spectrum.

To further investigate, we repeated the same analysis with limited samples of near-cloud pixels. Figure 4 (a) shows the plots for the same GLI data but for those pixels that are adjacent to any cloud pixel and have Chl-a value of "out of range (Chl-a < 0.01 or Chl-a > 10.0 µg/l)". In contrast, Figure 4 (b) is also the result of the same scene but with the pixels that are enough far (more than 5 pixels) from any cloud pixel and have "likely range of Chl-a (0.05 < Chl-a < 10.0 mg/l)". By comparison of these results, we can define a new scheme for screening those pixels with anomalous spectra to remove all the pixels that fall within the surrounding scattered area of the diagram.

3. EVALUATION OF THE PROPOSED METHOD

3.1 Definition of the method

We define here a "reference relationship" of between two inter-band reflectance ratios $IRR_1 = Rrs(443)/Rrs(520)$ and $IRR_2 = Rrs(460)/Rrs(545)$ as

$$\log_{10} IRR_2 = 0.865 \log_{10} IRR_1 + 0.184, \quad (3)$$

which was determined from the analysis of an 8 day global Level 2 data of GLI. Then, the new scheme, which we call "Inter-band Reflectance Consistency (IRC)" test, is described as follows.

3.2 IRC criteria

1) The pixel should meet the following condition,

$$Ref - 0.2 < \log_{10} IRR_2 < Ref + 0.2,$$

where Ref is the value of right-hand side of (3) based on the satellite-derived IRR1.

2) The pixel also should meet

$$0.1 < \log_{10} IRR_1 < 20, \text{ and } 0.1 < \log_{10} IRR_2 < 20.$$

The scheme for pixel-wise screening is to "mask" the pixel if it does not meet 1) and 2) at the same time.

3.3 Evaluation by comparison with local variance test

As one can expect, proposed IRC test masks less number of pixels around cloud compared to the local variance test. Figure 5 illustrates this nature, showing the results of different cloud screening methods applied to a South China Sea scene of April 3, 2003, where the three panels are Chl-a images with (a) simple threshold, with (b) simple threshold an additional local variance, with (c) simple threshold and additional IRC tests, respectively. As seen in the figure, the case (c) (simple threshold + IRC)

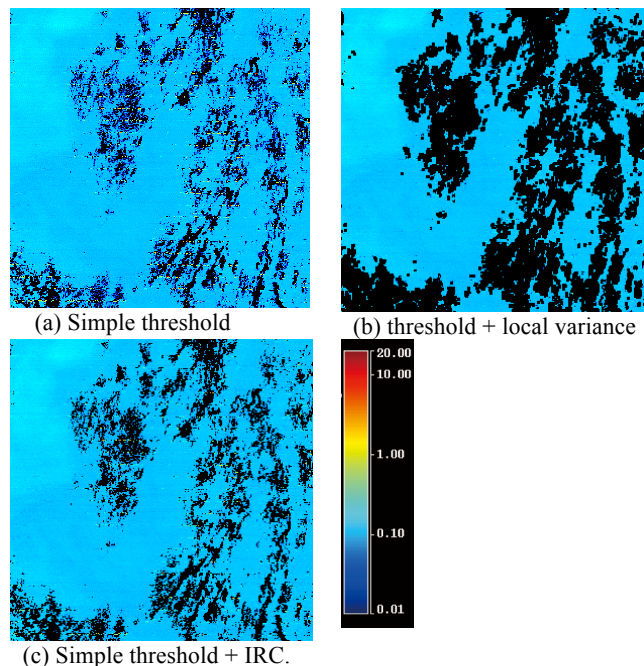
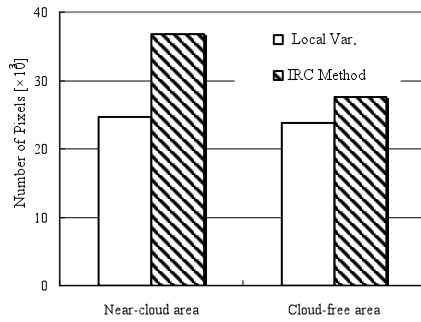
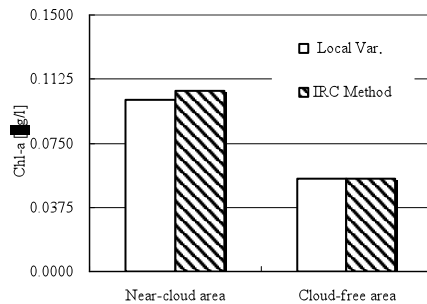


Figure 5. Performance of different cloud mask applied to South China sea Chl-a image of April 3, 2003.



(a) Number of available pixels



(b) Standard deviation of log[Chl-a]

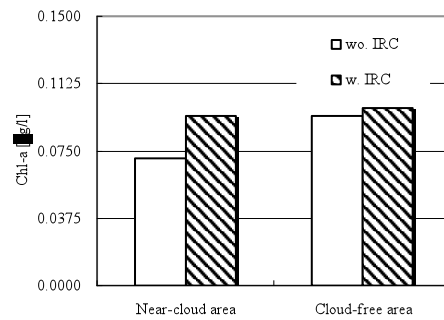
Figure 6. Cloud mask performance comparison between local variance and IRC methods.

obviously masks much less number of pixels compared to (b), yet masking significant portion of anomalous pixels seen on the cloud edge (in Figure 5 (a)).

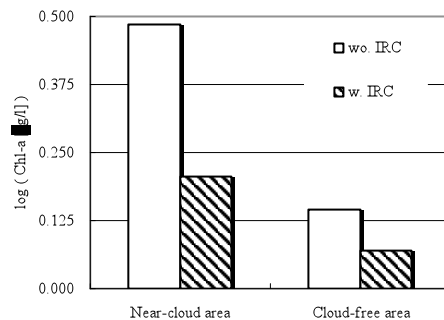
As a quantitative evaluation, we compared number of available (not cloud-masked) pixels for the local variance test and for the IRC test over “cloud edge” and “far-cloud” pixels for the South Pacific GLI image used in Figure 4 (Figure 6 (a)). From the results, IRC test produces about 50% more valid pixels in “Near-cloud” area compared to the local variance test, where a “Near-cloud” pixel is the one adjacent to any cloud pixel. Note that, as shown in Figure 6(b), the standard deviation in the near-cloud area under the two methods is just the same. This can be interpreted that the quality of the IRC cloud screening is just the same as the local variance method, although the difference in standard deviation between cloud edge pixels and far-cloud pixels may mean the necessity of further improvement of cloud screening tests.

3.4 Evaluation as an additional cloud screening test

We evaluated the performance of the proposed scheme as an additional cloud test to the standard GLI cloud screening, which consists of simple threshold/local variance tests and cloud-adjacent pixel masking. Figure 7 shows statistical results obtained under the GLI standard method (“wo. IRC”) and under the standard method with IRC test (“w. IRC”) for the South Pacific GLI scene of June 5, 2003. As seen in Figure 7(a), it is noteworthy that the modified method with IRC test gives just the same Chl-a average for cloud-edge and for far-cloud pixels. At the same time, the factor of 2 difference in standard deviation of Chl-a between cloud-edge and far-cloud pixels (Figure 7(b)) may necessitate further study.



(a) Chl-a average



(b) Standard dev. of log[Chl-a]

Figure 7. Cloud mask performance comparison between GLI standard method and modified IRC-added method.

4. CONCLUSION

We proposed a new cloud screening method that utilizes “inter-band consistency” of the water reflectance. It leaves more “near-cloud” pixels compared to “local variance” method while detecting dubious pixels just as the local variance method does. Although we have developed this method over GLI data, the technique is also applicable to other satellite ocean color data.

It might be pointed out that the method is based on the spectral nature of the “Case-I” waters where optical properties of the water is controlled only by phytoplankton, and hence the method may not work against some extraordinary environments such as red-tide, high-turbidity or coccolithophore blooms. While we propose this method as an additional cloud-screening algorithm as a part of the JAXA standard SGLI ocean color data processing, further studies should be conducted to enhance the applicability of the method over various water types and atmospheric conditions.

References

Fu, G., Baith, K. S., and McClain, C. R., SeaDAS: The SeaWiFS Data Analysis System, Proceedings of the 4th Pacific Ocean Remote Sensing Conference, Qingdao, China, July 28-31, 1998, 73-79. 1998.

Fukushima, H., M. Toratani, H. Murakami, P. Deschamps, R. Frouin, and A. Tanaka, Validation of ADEOII/GLI ocean color

atmospheric correction based on ship-board hand-held spectroradiometer measurements, Proc. of SPIE, 5885, 588505-1 – 588505-8, 2005.

Murakami, H., M. Yoshida, K. Tanaka, H. Fukushima, M. Toratani, A. Tanaka, and Y. Senga, Vicarious calibration of ADEOS/GLI visible to shortwave infrared bands using global datasets, Trans. Geosci. Rem. Sens., 43, 7, 1571-1584, 2005.

O'Reiley, J. E., S. Maritorena, B.G. Mitchell, D. A. Siegel, K. L. Carder, S. A. Garver, M. Kahru, C. McClain, Ocean color chlorophyll algorithms for SeaWiFS, J. Geophys. Res., 102, 24937-24953, 1998.

Acknowledgements

This work was supported by Japan Aerospace Exploration Agency (JAXA) under contract JX-PSPC-307627.